Clinical Ophthalmology

Dovepress
Taylor & Francis Group

Open Access Full Text Article

REVIEW

In vivo Confocal Microscopy for Corneal and Ocular Surface Pathologies: A Comprehensive Review

Arturo Ramirez-Miranda[1], Jesus Guerrero-Becerril[1], Manuel Ramirez[2], Guillermo Raul Vera-Duarte[1], Simran Mangwani-Mordani[1,3,4], Gustavo Ortiz-Morales[1], Alejandro Navas[1], Enrique O Graue-Hernandez[1], Jorge L Alio[5]

[1]Departamento de Córnea y Cirugía Refractiva, Instituto de Oftalmología Fundación Conde de Valenciana IAP, Mexico City, Mexico; [2]Departamento de Córnea y Cirugía Refractiva, Asociación para Evitar la Ceguera en México, Hospital Luis Sánchez Bulnes, Universidad Nacional Autónoma de México, Mexico City, Mexico; [3]Surgical Services, Department of Ophthalmology, Miami Veterans Affairs Medical Center, Miami, FL, USA; [4]Department of Ophthalmology, Bascom Palmer Eye Institute, University of Miami, Miami, FL, USA; [5]Research and Development Department, VISSUM Miranza, Alicante, Spain

Correspondence: Arturo Ramirez-Miranda, Instituto de Oftalmologia Fundacion Conde de Valenciana IAP, Chimalpopoca 14, Centro, Cuauhtémoc, Ciudad de México, CDMX, CP 06800, Mexico, Email arturorammir@gmail.com

Background: In vivo confocal microscopy (IVCM) is an advanced imaging technique that enables real-time, high-resolution visualization of corneal microstructures. Its clinical applications have expanded significantly, offering valuable insights into the pathophysiology of various ocular surface and corneal disorders. Despite its utility, challenges in standardization, accessibility, and integration into routine practice limit its widespread adoption.

Methods: A comprehensive literature review was conducted using PubMed with the keywords "in vivo confocal microscopy", "corneal diseases", and "ocular surface". From 1835 articles retrieved, studies published within the last seven years with clinical relevance were prioritized, yielding 51 articles. Data were synthesized to evaluate IVCM's diagnostic capabilities, technical advancements, and applications across corneal pathologies, including infectious keratitis, dystrophies, and post-surgical outcomes.

Results: IVCM was shown to provide unparalleled visualization of cellular and subcellular corneal structures, enabling early diagnosis and monitoring of conditions such as keratitis caused by Acanthamoeba and fungi, corneal dystrophies, and nerve regeneration following refractive or transplant surgeries. Innovative applications include its use in regenerative therapies, such as adipose-derived stem cell implantation, demonstrating increases in keratocyte density and stromal integrity. However, limitations include operator dependency, high costs, and the need for further technological refinements, such as wide-field imaging and non-contact modalities.

Conclusion: IVCM represents a transformative tool in ophthalmology, bridging the gap between clinical evaluation and cellular-level diagnostics. Advances in imaging technologies and the integration of artificial intelligence hold the potential to overcome current limitations, enhancing its diagnostic precision and applicability. Standardization of protocols and expanded access will be pivotal in establishing IVCM as a cornerstone in the management of corneal diseases and ocular surface disorders.

Keywords: In vivo confocal microscopy, IVCM, corneal imaging, ocular surface diseases, regenerative medicine, corneal nerves

Introduction

In vivo confocal microscopy (IVCM) is a non-invasive imaging technique that enables the microscopic examination of the cornea, providing ultra-structural analysis under normal conditions and in various hereditary and acquired pathologies.[1] The increasing interest in corneal cellular pathophysiology, along with advancements in IVCM, has established it as a valuable diagnostic tool for numerous ocular diseases.[2]

Several confocal microscopy systems are utilized in IVCM. The scanning-slit confocal microscope (Confoscan, Nidek, Fortune Technologies, Italy) uses vertical slit apertures for simultaneous illumination and field observation,

Received: 17 February 2025
Accepted: 28 May 2025
Published: 7 June 2025

significantly reducing examination time by scanning all points along the slit axis simultaneously. Adjustable slit height and width allow control over optical section thickness and light intensity, enhancing image brightness, contrast, and patient comfort.[3,4] The system achieves a "Z" axis resolution of up to 1 μm and captures up to 350 images per scan, with a pixel spacing of approximately 0.56 μm horizontally and vertically. The "Z ring scan" device minimizes anterior-posterior movement, facilitating precise depth measurements.[5]

The latest generation of IVCM, represented by the Heidelberg Retina Tomograph 2 with the Rostock Corneal Module (HRT 2-RCM, Heidelberg Engineering GmbH, Germany), offers high-definition images comparable to histological corneal sections, with an axial resolution of approximately 4 μm—significantly better than the 10 μm of conventional confocal microscopy.[2,6] In this system, both the condenser and objective lenses focus on a small tissue area simultaneously, characterizing it as confocal microscopy.[1] The HRT 2-RCM is preferred for clinical research due to its high resolution and advanced analysis software, despite its high cost and the need for specialized training. In contrast, the Nidek Confoscan 4, while less expensive and more suitable for corneal nerve studies and cell density measurements, has a lower resolution and less intuitive interface. The CellCheck XL from Konan Medical, specializing in corneal endothelial cell evaluations, offers precise measurements but limited applications. Therefore, selecting the appropriate IVCM technology requires careful consideration of each device's strengths and limitations to optimize ophthalmic care.

This review examines the current uses and diverse applications of IVCM in corneal and ocular surface diseases.

Historical Background

Since the 1990s, confocal microscopy has been widely utilized in various scientific fields, including biomedical research, cellular biology, material sciences, and industry applications. Technological advancements have enabled real-time imaging of biological tissues in vivo. The first in vivo images of the human cornea were obtained in 1989 by Cavanaugh et al.[7] Later, Masters and Thaer demonstrated the use of confocal microscopy for capturing live images of the human cornea, reinforcing its significance in ophthalmology.[2,6,8]

Anatomy of the Tear Film and Cornea

IVCM is used to evaluate tear film quality through high-resolution imaging, enabling correlations between tear break-up time and its morphological representation (Figure 1). Tandem scanning confocal microscopy captures real-time images, including "dry spots", but its primary use remains research-oriented due to high costs and operator dependency.[9] IVCM provides uniform illumination of all corneal layers, including the epithelium, corneal nerves, keratocytes, and endothelium. The hydraulic Z-axis scanning feature of the Heidelberg Retina Tomograph (HRT) with the Rostock Corneal

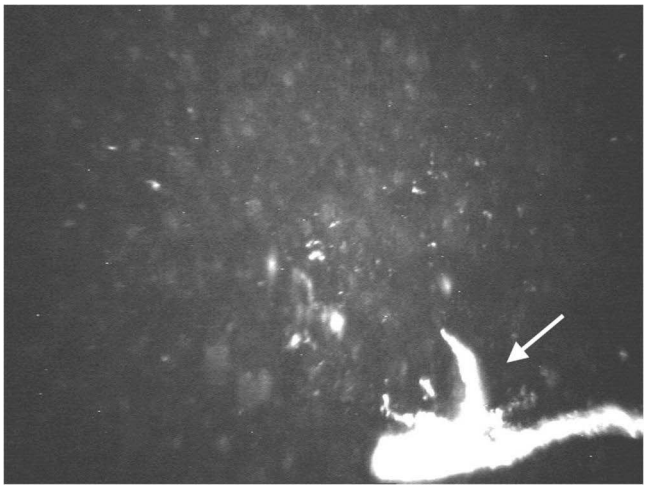

Figure 1 Confocal microscopy image showing an irregular, hyperreflective structure in the lower right corner corresponding to mucin accumulation in a patient with dry eye (340 × 255 μm). The white arrow indicates the interface between the dense mucin deposit and adjacent epithelial cells, highlighting the abrupt reflectivity transition characteristic of abnormal mucin pooling.

Module (RCM) allows precise transitions between layers, capturing cellular series and generating 3D images of corneal structures.[9,10]

The corneal epithelium acts as a barrier against pathogens, maintaining ocular surface homeostasis. In healthy individuals, epithelial cell density ranges from 1026 to 1398 cells/mm² and 1299 to 1758 cells/mm² (Figure 2).[11] Basal cell density varies between 5168 to 6348 cells/mm² and 11,307 ± 1876 cells/mm² (Figure 3).[11,12] Wing cells, less visible on IVCM, can still be identified by their bright edges and nuclei.[11,12] The cornea is one of the most densely innervated tissues, with nerves forming the subbasal plexus, a key feature captured effectively by HRT-RCM.[11–14] Temporal changes in the subbasal plexus during disease or post-surgery have been documented (Figure 4), as well as long and deep nerve visualization (Figure 5).[14,15] However, IVCM's limitations in capturing fine nerve endings may explain the inconsistent correlation between nerve loss and reduced corneal sensitivity in some studies.[14,15]

To assess corneal nerve patterns, parameters such as nerve length, density, tortuosity, and vortex length are considered. Nerve fiber length, sensitive to neuropathy, ranges from 3.9–27.5 mm/mm².[14] Nerve density (fibers/mm²) has been evaluated in systemic conditions, showing a negative correlation with HbA1c levels.[14,16] Post-LASIK, nerve density decreases, with regeneration signs appearing within a month (Figure 6).[17] Increased nerve tortuosity has been

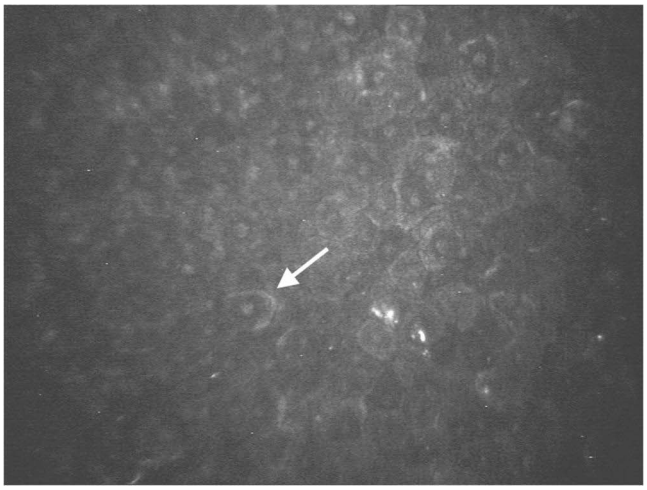

Figure 2 Confocal microscopy image of the superficial corneal epithelium (340 × 255 μm). The arrow highlights a desquamating epithelial cell, identifiable by its irregular borders and increased reflectivity, consistent with superficial epithelial cell turnover commonly seen in dry eye disease.

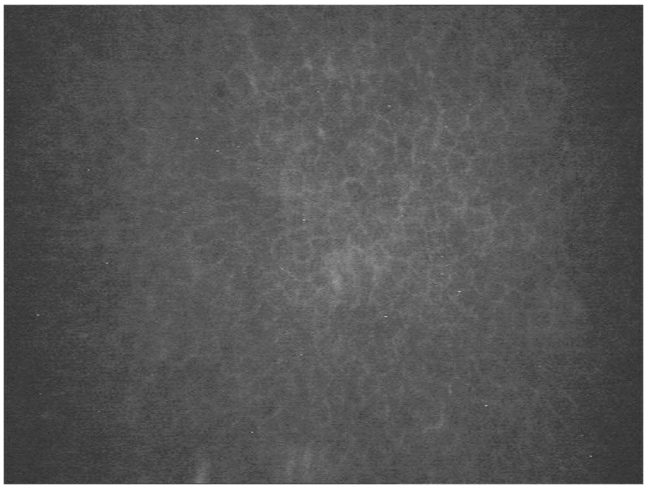

Figure 3 Confocal microscopy image of the basal epithelial cells (340 × 255 μm).

https://doi.org/10.2147/OPTH.S519705

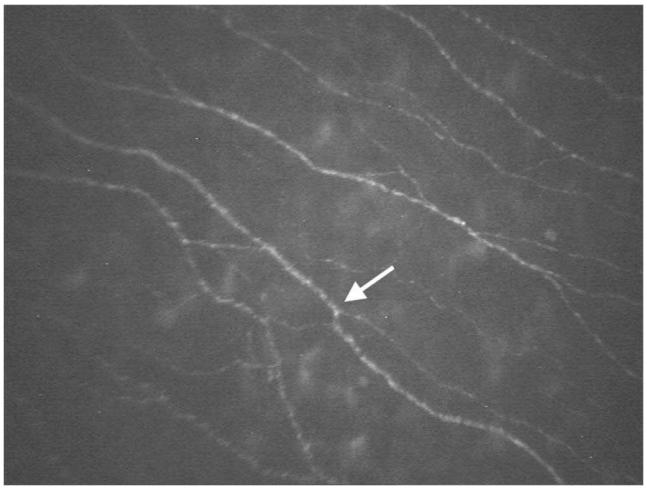

Figure 4 Confocal microscopy image of the subepithelial nerve plexus (340 × 255 μm). The arrow points to a beaded nerve fiber, indicating the presence of varicosities typically associated with increased nerve activity or regenerative changes in the corneal subbasal nerve plexus.

Figure 5 Confocal microscopy image of the mid-corneal stroma showing a stromal nerve with its characteristic linear appearance (340 × 255 μm). The arrow indicates a segment of the nerve fiber, emphasizing its uniform reflectivity and trajectory through the stromal matrix.

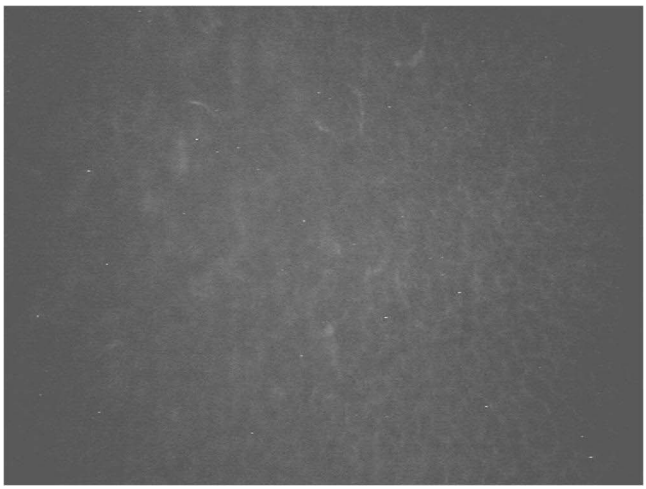

Figure 6 Confocal microscopy image of a patient one week after LASIK surgery showing the absence of the subepithelial nerve plexus (340 × 255 μm).

noted in conditions like keratoconus, pseudoexfoliation syndrome, Sjögren's syndrome (SS), rheumatoid arthritis (RA), and after penetrating keratoplasty (PKP).[14]

In Bowman's layer, IVCM reveals polymorphic "K structures" (fibrillar material likely representing condensed collagen) and ridges from basal and wing cells.[18] The corneal stroma is well visualized with IVCM, showing a good correlation between keratocyte density in vivo and ex vivo (Figure 7). Under normal conditions, only keratocyte nuclei are visible; during wound healing, they appear hyperreflective with poorly defined processes, indicating keratocyte activation (Figure 8).[1] Variability in density reports may result from differences in resolution, contrast, or stromal definition.

Descemet's membrane appears as an acellular layer, often indistinguishable by IVCM.[1] Corneal endothelial density measured by IVCM correlates well with specular microscopy, even in moderate corneal edema cases (Figure 9).[1] To measure corneal thickness, IVCM generates intensity curves (285 x 285 μm resolution), plotting peaks corresponding to the epithelium, subbasal plexus, and endothelium. Thickness is calculated from the first peak (endothelium) to the last peak (epithelium).[19]

Compared to Scheimpflug tomography and ultrasonic pachymetry, IVCM overestimates thickness by 14 μm and 5 μm, respectively.[20]

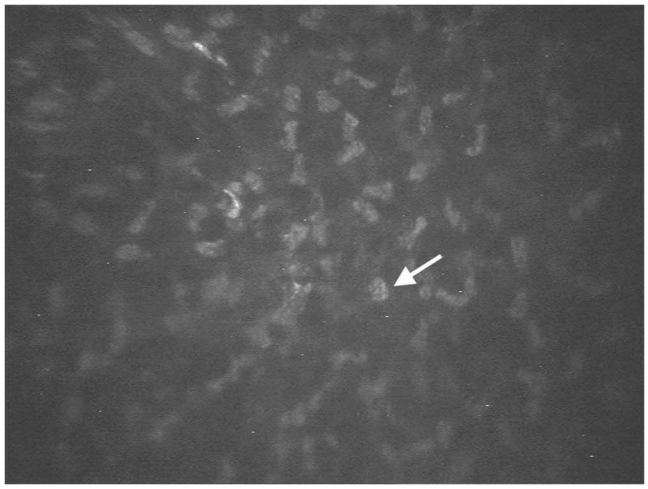

Figure 7 Confocal microscopy image of anterior stromal keratocyte nuclei under normal conditions (340 × 255 μm). The arrow indicates a representative keratocyte nucleus, characterized by its oval shape and moderate reflectivity, typical of quiescent stromal cells in a healthy cornea.

Figure 8 Confocal microscopy image showing activated keratocytes with visible cytoplasm and hyperreflective nuclei in the mid-stroma of a post-LASIK patient (340 × 255 μm). The arrow highlights a cluster of activated keratocytes, identifiable by their enlarged, irregular shapes and increased reflectivity, indicative of stromal wound healing activity.

https://doi.org/10.2147/OPTH.S519705

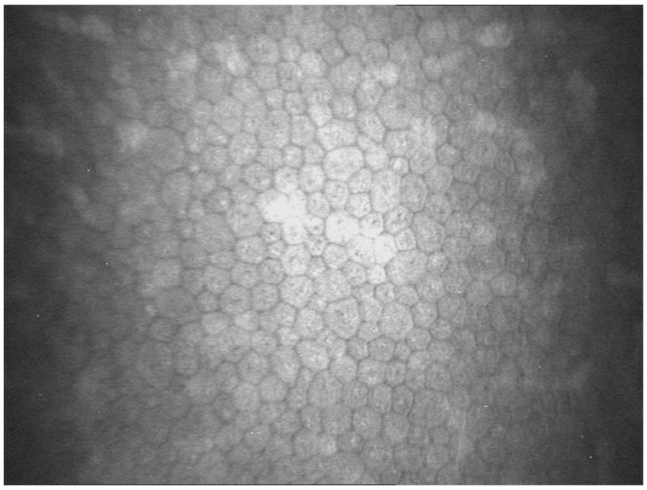

Figure 9 Confocal microscopy image of the corneal endothelium under normal conditions (340 × 255 μm).

Alterations in Corneal Pathologies

Meibomian Gland Dysfunction

The HRT-RCM facilitates microscopic evaluation of various palpebral and ocular surface structures, including the eyelid, conjunctiva, cornea, limbus, tarsal conjunctiva, and Meibomian glands. For Meibomian gland analysis, coronal scanning through the acinar mass posterior to a vertically oriented duct is performed. In IVCM, Meibomian gland acini appear as lobulated structures with circumvoluted borders, with cells lining the acini and fine cellular material inside.[21]

Age-related changes include reduced acinar density, homogeneity, and meibum quality.[21,22] In Meibomian gland dysfunction (MGD), acinar ducts become dilated and obstructed.

Dry Eye Syndrome

Dry eye syndrome (DES) encompasses various clinical manifestations, including ocular surface dryness, pain, fluctuating vision, and blurred vision, significantly impacting quality of life.[23] The Tear Film and Ocular Surface Society International Dry Eye Workshop II (TFOS DEWS II) defines dry eye as "a multifactorial disease of the ocular surface characterized by a loss of tear film homeostasis accompanied by ocular symptoms, with tear film instability, inflammation, ocular surface damage, and neurosensory abnormalities playing etiological roles".[24] Due to the nonspecific symptoms of DES, targeted treatments are challenging, prompting the use of advanced technologies like IVCM to investigate pathophysiological changes.

IVCM has revealed numerous findings in Sjögren's syndrome (SS). Studies have shown significantly lower epithelial cell density in SS patients (741 ± 306 to 971 ± 262 cells/mm² and 965.4 ± 96.0 to 993.1 ± 104.8 cells/mm²) compared to healthy controls (1431 ± 283 to 1528 ± 341 cells/mm² and 1485.6 ± 133.7 to 1511.6 ± 136.0 cells/mm²).[21,22,25–27] However, changes in basal and wing cell density in DES remain unclear. Increased stromal cell density has also been observed in SS patients. One study reported a significant increase in dendritic cell density in the corneal epithelium of non-Sjögren and SS dry eye patients compared to healthy individuals (non-SS: 89.8 ± 10.8 cells/mm²; SS: 127.9 ± 23.7 cells/mm²; control: 34.9 ± 5.7 cells/mm²).[28] (Figure 10)

IVCM has also been used to analyze epithelial, inflammatory, endothelial cells, keratocytes, and stromal nerves in DES patients. Studies have particularly focused on changes in the density and morphology of subbasal nerves and dendritic cells. Contrary to findings in aqueous tear deficiency, evaporative dry eye patients show no significant differences in nerve plexus density compared to healthy controls. Two studies reported no differences in fiber density (27.20 ± 0.60 vs 28.60 ± 0.80 nerves/mm²; $p > 0.05$ and ~30 nerves/mm² in both groups; $p > 0.05$).[29,30]

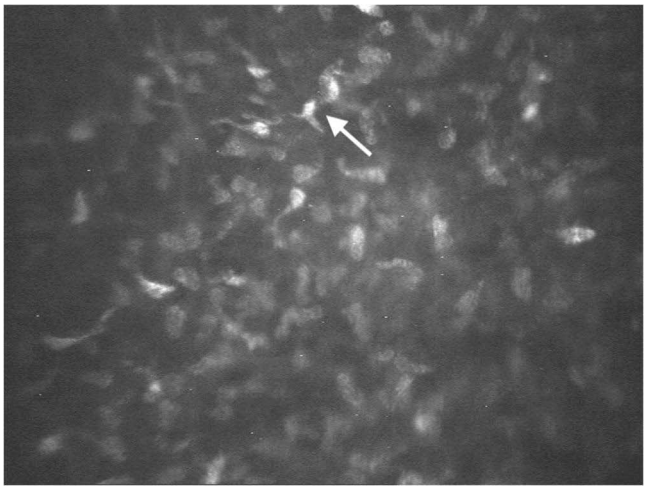

Figure 10 Confocal microscopy image of the anterior corneal stroma in a patient with dry eye, showing moderate keratocyte activation (340 × 255 μm). The arrow points to a representative activated keratocyte, noted for its increased reflectivity and slightly enlarged, irregular shape compared to quiescent stromal cells.

Corneal Nerves (CN)

Corneal nerves (CN) originate from the ophthalmic division (V1) of the trigeminal nerve, primarily the nasociliary nerve, and branch into the cornea.[21,22,25,31] Beyond sensory functions, CNs stimulate tear production through the lacrimal functional unit and promote trophic factor release, which, together with the tear film, maintains ocular surface integrity.[31,32] Neuronal damage disrupts ocular surface homeostasis, leading to epithelial compromise, a cycle of inflammation, and anatomical or functional changes detectable with IVCM.[11,31,32]

Oliveira-Soto and Efron[33] were among the first to use IVCM to characterize CNs, developing grading scales for tortuosity and reflectivity. They identified four main plexiform nerve layers based on corneal involvement: mid-stroma, anterior-mid, anterior, and subbasal epithelial layers.[33] Each plexus differs in thickness, density, tortuosity, and reflectivity. The subbasal plexus, located between Bowman's layer.

Limbal Stem Cell Deficiency (LSCD)

Limbal stem cell deficiency (LSCD) can arise from various ocular conditions, including chemical injuries, repeated intraocular surgeries, and Stevens-Johnson syndrome.[34] Diagnosing and managing LSCD remains challenging, with impression cytology and IVCM being valuable diagnostic tools.[35] In advanced LSCD, IVCM reveals morphological changes, hyperreflective cellular nuclei, intraepithelial cystic lesions with goblet cells, and epithelial thinning.[34,36–38]

In partial LSCD, even seemingly unaffected areas may show similar changes, suggesting a potential preclinical detection method.[39,40] Zarei-Ghanavati et al[41] identified a novel limbal structure via IVCM termed the "limbal lacuna", containing normal limbal epithelial cells within the stromal limbus. This structure, absent in Vogt's palisades in sectoral LSCD, may serve as a resilient niche for limbal stem/progenitor cells.

Langerhans dendritic cells (DCs), the primary antigen-presenting cells (APCs) in the corneal epithelium, typically reside in the subbasal plexus, predominantly at the periphery. During inflammation, DC hyperplasia and migration toward the central cornea are observed.[28]

Reduced corneal nerve (CN) density has been reported in aqueous tear deficiency. Erie et al found significantly lower nerve density in patients with tear deficiency (9426 ± 2640 vs 15,956 ± 2431 μm/mm; $p < 0.0001$).[32,42,43] Similarly, Choi et al[44] reported decreased nerve density (9884 ± 2548 vs 12,030 ± 2203 μm/mm²; $p < 0.005$) and increased tortuosity (3.70 ± 0.50 vs 1.60 ± 0.60; $p < 0.001$) in dry eye patients. Not all studies have quantified changes in nerve density; some report reduced nerve count instead. Two studies found a decrease in nerve count in dry eye patients compared to healthy controls (34.91 ± 8.08 vs 45.87 ± 4.21 nerves/mm², $p < 0.001$; 3.90 ± 0.50 vs 5.80 ± 1.30 nerves/frame, $p < 0.001$).[43,45] (Figure 11)

https://doi.org/10.2147/OPTH.S519705

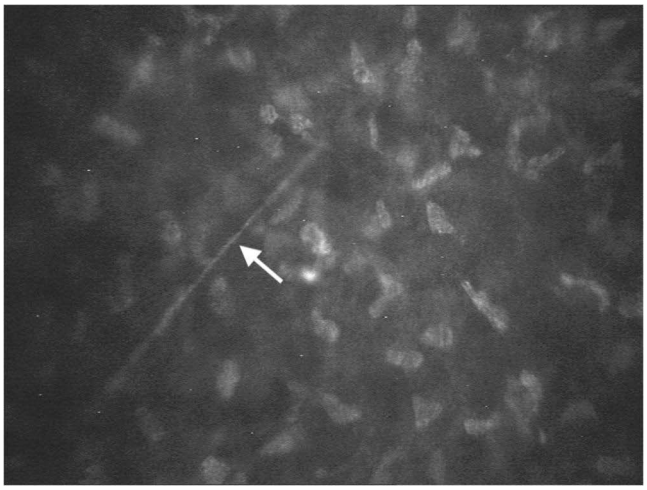

Figure 11 Confocal microscopy image showing a thin stromal nerve in the mid-stroma of a patient with fibromyalgia (340 × 255 μm). The arrow identifies the stromal nerve, visible as a faint, linear hyperreflective structure, which may reflect small fiber involvement commonly reported in systemic pain syndromes.

Sjögren's Syndrome

Extensive IVCM studies in Sjögren's syndrome (SS) have demonstrated significantly lower epithelial cell densities in SS patients compared to healthy controls.[21,22,25] Increased stromal cell density has also been reported in SS patients (741 ± 306 to 971 ± 262 cells/mm² and 965.4 ± 96.0 to 993.1 ± 104.8 cells/mm²) versus healthy individuals (1431 ± 283 to 1528 ± 341 cells/mm² and 1485.6 ± 133.7 to 1511.6 ± 136.0 cells/mm²).[21,22,25–27] Changes in basal and wing cell densities in dry eye syndrome remain unclear, but increased stromal cell density is consistently reported in SS cases. (Figure 10) Nerve abnormalities in SS-associated dry eye have been extensively studied, showing similar patterns to aqueous-deficient dry eye, including reduced nerve density and increased tortuosity. Villani et al[26] reported significantly fewer nerves in SS dry eye patients compared to healthy controls (3.34 ± 0.76 vs 5.10 ± 0.79 nerves/frame, $p < 0.0001$). Other studies[46] noted decreased plexus density and fewer nerves in SS patients compared to controls (3.18 ± 0.75 vs 1.09 ± 0.54, $p < 0.0001$). In contrast, Zhang et al[46,47] found a higher number of corneal nerves (8.80 ± 1.30 vs 6.30 ± 3.10 nerves/frame, $p = 0.03$) and increased tortuosity (3.10 ± 0.80 vs 2.20 ± 0.90, $p = 0.02$) in SS patients, although changes in plexus density were not statistically significant (1745.40 ± 414.70 vs 1315.70 ± 664.70 μm/frame, $p = 0.09$). Regarding dendritic cells (DCs), significantly increased DC density in the corneal epithelium has been noted in both non-SS and SS dry eye patients compared to healthy controls (non-SS: 89.8 ± 10.8 cells/mm²; SS: 127.9 ± 23.7 cells/mm²; controls: 34.9 ± 5.7 cells/mm²).[28]

Ocular Graft-Versus-Host Disease (oGVHD)

Ocular graft-versus-host disease (oGVHD) is an inflammatory condition that affects the subbasal plexus,[48] though the impact on corneal structures remains debated due to conflicting study results. Two studies compared non-GVHD dry eye patients to those with GVHD-associated dry eye, analyzing epithelial cell count, dendritic cell (DC) density, and subbasal plexus density, but found no statistically significant differences between the groups.[49,50] In contrast, Steger et al[51,52] reported a significant reduction in CN density in oGVHD patients compared to controls (11,220 ± 5460 vs 19,560 ± 4750 μm/mm², $p < 0.01$). Tepelus et al[52] found no significant difference in nerve tortuosity (2.23 ± 0.69 vs 2.16 ± 0.43, $p > 0.05$), while other studies reported increased tortuosity (2.8 ± 1.1 vs 1.3 ± 0.5, $p < 0.001$). Despite analyzing DC counts across four studies, no significant differences emerged when comparing GVHD ocular patients, non-GVHD dry eye patients, and healthy controls. Although IVCM findings in GVHD patients are not specific to oGVHD, the technique may be valuable for the early subclinical detection of subbasal plexus inflammation, potentially indicating subsequent clinical deterioration.

Ocular Neuropathic Pain

In some patients, discrepancies exist between reported symptoms and observed clinical signs on the ocular surface.[51,53] Neuropathic pain is often described as "stabbing", "burning", "tingling", or "itching", and may include allodynia (pain triggered by non-painful stimuli like light or wind) and hyperalgesia (exaggerated pain responses).[23,51,53] Risk factors for ocular neuropathic pain include surgeries (eg, refractive surgery), infections (eg, herpes), and systemic diseases (eg, fibromyalgia). Hamrah et al[54] visualized the subbasal nerve plexus in patients with ocular neuropathic pain, reporting reduced nerve density compared to healthy controls. Structural abnormalities, such as reduced nerve length, density, and diameter, have been noted in fibromyalgia patients (Figure 11).[23,55,56] Similarly, migraine patients show significantly lower subbasal nerve density than healthy individuals.[23,57]

Aggarwal et al[58] identified microneuromas (terminal bulbs with small branches at axonal injury sites attempting regeneration) in patients with ocular neuropathic pain, a finding not observed in healthy controls. A study comparing neuropathic pain, dry eye, and healthy controls found reduced subbasal nerve plexus density in both neuropathic pain and dry eye groups compared to controls (14.14 ± 1.03 mm/mm², 12.86 ± 1.04 mm/mm², and 23.90 ± 0.92 mm/mm², respectively; $p < 0.001$), although nerve density did not significantly differ between neuropathic pain and dry eye patients ($p = 0.63$). Microneuromas were present in all neuropathic pain patients but absent in dry eye patients, showing 100% sensitivity and specificity.[59] DC density was significantly higher in neuropathic pain (71.89 ± 16.91 cells/mm²) and dry eye (111.5 ± 23.86 cells/mm²) compared to controls (24.81 ± 4.48 cells/mm², $p < 0.05$).[59]

Another study stratified ocular neuropathic pain patients by response to topical anesthesia (responders [RG] vs non-responders [NRG]) compared to healthy controls. Patients with somatosensory dysfunction had significantly lower subbasal nerve density compared to controls (16.17 ± 4.1 mm/mm² vs 20.1 ± 4.3 mm/mm²; $p < 0.008$).[60] Corneal epithelial thickness did not differ significantly between groups (40.6 ± 5.3 µm vs 48.6 ± 8.9 µm; $p = 0.144$). All patients exhibited corneal stromal microneuromas, with fewer microneuromas in RG compared to NRG (9.3 ± 2.8 vs 2.95 ± 1.15; $p < 0.0001$). Differences in subbasal nerve density (RG: 17.56 ± 3.91 vs NRG: 16.80 ± 4.21; $p = 0.333$) and epithelial thickness (RG: 43.43 ± 5.99 µm vs NRG: 45 ± 5.1 µm; $p = 0.521$) were also not significant.[60]

These studies demonstrate reduced subbasal nerve plexus density in patients with neuropathic pain and dry eye compared to controls. The presence of microneuromas strongly suggests ocular neuropathic pain. However, structural changes detected via IVCM do not effectively differentiate between dry eye and somatosensory dysfunction.

Contact Lens Use

IVCM has been utilized to evaluate corneal changes associated with prolonged contact lens (CL) wear. Studies have reported a reduction in epithelial thickness among long-term CL users.[61] IVCM has also identified hypoxia-related changes, including hyperreflective keratocyte nuclei, increased epithelial cell size, decreased keratocyte density, accumulation of highly reflective stromal microdot deposits, and formation of endothelial cell layer blebs.[62–64]

These findings demonstrate the potential of IVCM as a diagnostic tool to monitor the impact of contact lens use on corneal health, facilitating early detection of adverse changes and guiding clinical management.

Corneal Ectasia

Keratoconus, the most common corneal ectasia, is characterized by conical corneal deformation, leading to irregular astigmatism, myopia, and reduced visual acuity.[65] IVCM has revealed cellular changes in keratoconus patients, including keratocyte nuclear elongation, anterior stromal keratocyte accumulation, hyporeflective bands in the posterior stroma, and thickened stromal nerves, with more pronounced alterations in advanced cases.[66,67]

A recent study comparing keratoconus and post-LASIK ectasia (PLE) using IVCM found that PLE patients exhibited vertically or slightly obliquely oriented nerves, unlike non-ectatic controls. Both keratoconus and PLE patients showed reduced subbasal plexus density compared to healthy controls, while endothelial density remained unaffected.[65,68]

Corneal Dystrophies

Corneal dystrophies are hereditary disorders characterized by bilateral, symmetrical, and slowly progressive changes. Anatomically, they are classified based on the affected corneal layer: epithelial and subepithelial, Bowman's membrane, anterior stromal, posterior stromal/Descemet's membrane, and endothelial dystrophies.[66,69] IVCM has emerged as a valuable tool for diagnosing corneal dystrophies by providing detailed cellular-level morphology.

Epithelial Dystrophies

In basement membrane dystrophy (map-dot-fingerprint dystrophy), IVCM shows thickened, highly reflective linear tissue in the basal epithelial layers, along with drop-shaped cysts (10 to 400 μm).[69] Meesmann's corneal dystrophy presents as hyporeflective epithelial areas with fragmented subbasal plexus.[1,69]

Bowman's Membrane Dystrophies

Reis-Bücklers dystrophy (Bowman's layer dystrophy type 1) features dystrophic deposits posterior to the basal lamina and highly reflective material in Bowman's layer.[1,69] Thiel-Behnke corneal dystrophy (Bowman's layer dystrophy type 2) shows pathological material replacing Bowman's layer, with rounded deposits and adjacent shadows.[69]

Stromal Dystrophies

Lattice corneal dystrophy is marked by amyloid deposits forming branched, hyperreflective structures.[69] Granular corneal dystrophy shows breadcrumb-like deposits (50 μm) in the epithelium and stroma, with a zone of unaffected tissue near the limbus.[1] (Figure 12) Schnyder's crystalline corneal dystrophy presents needle-like or rectangular crystalline deposits at Bowman's membrane and anterior stroma.[69,70] Macular corneal dystrophy displays striped deposits throughout the stroma.[71] Avellino dystrophy shows irregular granular material in the anterior and middle stroma, without affecting surrounding structures.[69,71]

In pre-Descemet's corneal dystrophy, IVCM visualizes intra- and extracellular inclusions (30–80 μm) anterior to Descemet's membrane.[69,71,72] Stromal fleck dystrophy features hyperreflective spots (1–18 μm) scattered throughout the stroma, resembling cystic structures.[69,71–74] Francois' central cloudy dystrophy presents as dense central opacities, with reflective stromal granules observed via IVCM.[73] Amorphous posterior corneal dystrophy reveals microfolds and peak-like posterior stromal extensions.[75]

Endothelial Dystrophies

Fuchs endothelial dystrophy is the most common endothelial dystrophy.[76] IVCM identifies round, hyporeflective areas with enhanced corneal endothelium reflectivity, pleomorphism, and polymegathism. Stromal edema is evident as

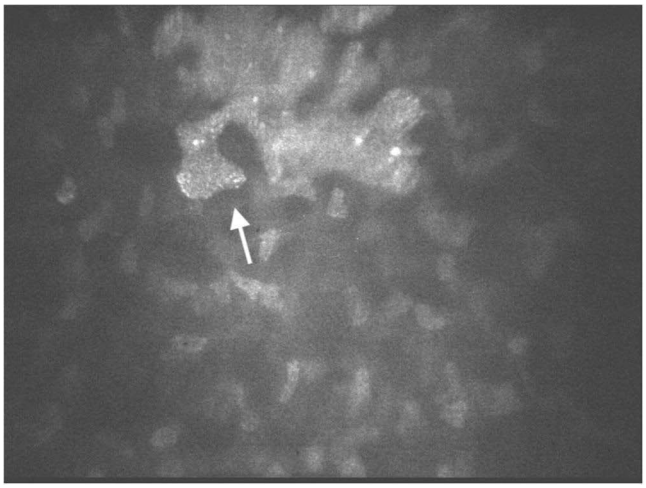

Figure 12 Confocal microscopy image showing granular dystrophy deposits in the mid-stroma (340 × 255 μm). The arrow highlights a well-defined hyperreflective deposit with irregular borders, characteristic of hyaline accumulations typically seen in granular corneal dystrophy.

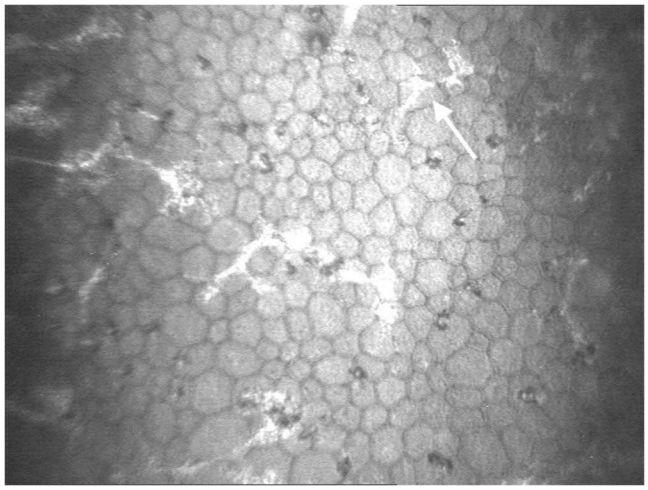

Figure 13 Confocal microscopy image of the corneal endothelium in a patient with Fuchs' dystrophy. (340 × 255 μm).The arrow highlights a gutta, seen as a localized dark area surrounded by hyperreflective borders, characteristic of endothelial cell loss and Descemet membrane excrescences in Fuchs' endothelial dystrophy.

darkened lamellae, with black bands (Descemet's folds) and fluid clusters.[77] (Figure 13) Posterior polymorphous corneal dystrophy is characterized by craters, grooves, and fissures on the endothelial surface, with vesicular lesions appearing doughnut-shaped.[77,78]

Infectious Keratitis

Microbiological diagnosis via corneal scraping remains the gold standard for infectious keratitis. However, IVCM has emerged as a valuable adjunct, particularly for slow-growing organisms like Acanthamoeba or fungi. Studies by the American Academy of Ophthalmology have provided Level II evidence supporting the use of IVCM in diagnosing Acanthamoeba keratitis.[79,80] Infectious keratitis is a leading cause of corneal blindness, and accurate diagnosis is essential for early intervention.[81] IVCM is increasingly used due to its rapid, high sensitivity in detecting larger organisms, such as filamentous fungi, Acanthamoeba, and Nocardia.[81]

Bacterial Keratitis

Bacteria are generally smaller than the resolution of IVCM, but larger bacteria (1.5 μm) have been imaged. Case reports have documented IVCM appearances of infections caused by Borrelia, Microsporidia, Streptococcus viridans, and Staphylococcus warneri.[82–84] IVCM findings in infectious crystalline keratitis include needle-like or amorphous deposits at various stromal depths, although no correlation with culture results was observed.[85] Additionally, clusters of neutrophils and lymphocytes have been identified as potential markers for bacterial keratitis, but more studies are needed to establish definitive criteria.[86,87]

Acanthamoeba Keratitis

Acanthamoeba keratitis is a rare, often misdiagnosed condition linked to contact lens use. Early diagnosis is crucial as delays worsen visual outcomes and increase surgical intervention rates.[1,60] IVCM can detect Acanthamoeba cysts and trophozoites: cysts appear as highly refractile, round or oval bodies with double walls (10–15 μm), while trophozoites are larger (25–40 μm) and oval.[81,88] (Figure 14) Differentiating trophozoites from keratocyte nuclei can be challenging in inflamed corneas.[1]

IVCM has also visualized inflamed stromal nerves and small, irregular, hyperreflective elements (5–15 μm) in the basal epithelium, possibly representing cellular debris or altered cysts.[89] IVCM shows potential in monitoring treatment response, as trophozoites may not be visible four to six weeks after therapy begins. Despite its utility, corneal scraping or biopsy remains the definitive diagnostic method.[1]

https://doi.org/10.2147/OPTH.S519705

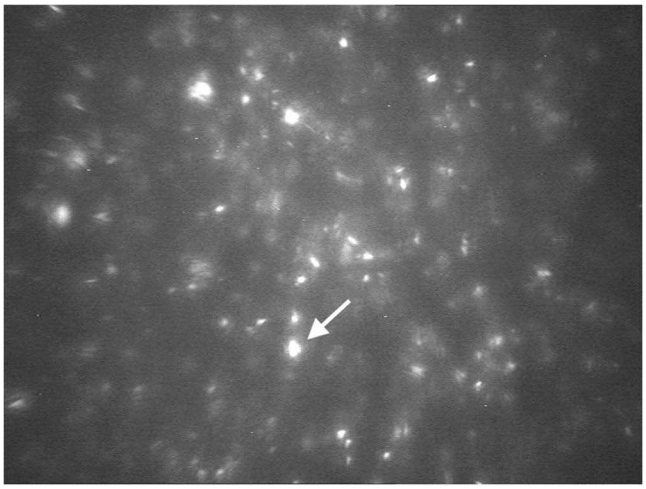

Figure 14 Confocal microscopy image showing Acanthamoeba cysts in the anterior stroma (340 × 255 μm). The arrow points to a characteristic Acanthamoeba cyst, identifiable by its double-walled, highly reflective round structure, aiding in the diagnosis of Acanthamoeba keratitis.

Fungal Keratitis

IVCM is less established for fungal keratitis, but case reports describe infections caused by Aspergillus, Fusarium, Beauveria, and Candida. Fungal hyphae appear as linear, hyperreflective, well-defined structures (width ~6 μm) with extensive branching.[90] Fungal elements can resemble double-walled structures and are seen as hyperreflective, branching lines (3–8 μm). Sensitivity and specificity have been reported as 94% and 74%, respectively.[1,81]

Corneal Surgical Procedures

Refractive Surgery

LASIK

Laser-assisted in situ keratomileusis (LASIK) involves cutting corneal nerves during flap creation. Studies have shown significantly lower subbasal nerve plexus density in LASIK-treated eyes compared to healthy controls, with reduced nerve branching density persisting even ten years post-surgery.[91] Hyperreflective particles have been observed at the corneal flap interface, and wing cell nuclei appear hyperreflective between 2 and 16 weeks post-LASIK.[92] (Figure 15A) Femtosecond laser and Hansatome microkeratome flaps show similar reflective particles.[90,92] Post-LASIK folds can extend from the basal epithelium to the stromal flap, penetrating deeper than Bowman's layer.[93]

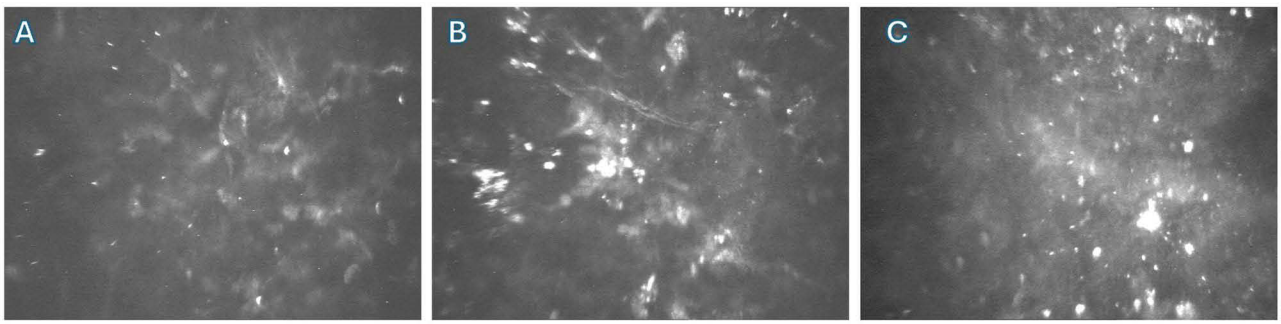

Figure 15 (**A**) Hyperreflective particles in the LASIK interface (340 × 255 μm). (**B**) Hyperreflective particles in the SMILE interface (340 × 255 μm). (**C**) Hyperreflective particles in the DALK interface (340 × 255 μm).

Photorefractive Keratectomy (PRK)

PRK involves epithelial removal and excimer laser ablation. IVCM shows the absence of Bowman's membrane at 10 and 20 years post-PRK, with persistent visibility of the subbasal nerve plexus. Ten years post-surgery, reduced keratocyte density is evident compared to healthy controls, with recovery occurring within six months.[94,95]

Small Incision Lenticule Extraction (SMILE)

SMILE corrects myopia and astigmatism via a femtosecond laser-generated lenticule. IVCM reveals an interface with absent keratocytes and hyperreflective particles. One week postoperatively, abnormally large keratocytes and a hyperreflective line appear.[96] (Figure 15B) SMILE shows higher nerve density compared to Femto-LASIK from one week to three months post-op, but differences diminish by six months.[97–99] Ramírez et al[100] reported accurate measurements of lenticule thickness and stromal interface depth.

Corneal Crosslinking (CXL)

In keratoconus patients treated with CXL, IVCM shows anterior and mid-stroma keratocyte loss, appearing as "honeycomb sponge-like edema" with hyperreflective apoptotic bodies and needle-like bands.[101]

Corneal Transplantation

Penetrating Keratoplasty (PKP)

PKP is associated with reduced subbasal nerve plexus density, as well as lower keratocyte and endothelial cell densities compared to healthy controls. Anterior stromal nerve regeneration occurs in 53% of patients within one year post-transplantation.[102]

Deep Anterior Lamellar Keratoplasty (DALK)

In deep anterior lamellar keratoplasty (DALK), an endothelial and Descemet-free graft is transplanted. IVCM has identified the interface between the donor graft and recipient tissue, described as a hyperreflective layer adjacent to the endothelium with small hyperreflective cysts. Keratocyte nuclei have been identified on the donor side of the interface.[103] (Figure 15C)

Endothelial Keratoplasty

This technique replaces the recipient's endothelium and Descemet's membrane. IVCM can visualize Bowman's membrane, the subbasal plexus, and normal endothelium post-transplant. Following DSAEK, IVCM reveals an average interface depth of 114 ± 12.4 μm and activated keratocytes up to seven weeks post-surgery.[104]

Corneal Regenerative Surgery

Corneal regenerative surgery is advancing treatment for keratoconus, dystrophies, and scars through bioengineering and cell therapy.[105] IVCM has been vital in monitoring these interventions, showing increased stromal cell density at implantation sites and suggesting potential keratocyte differentiation.[106–108]

One technique involves implanting autologous adipose-derived stem cells (ADASCs) into the corneal stroma, demonstrating safety and efficacy. IVCM shows stromal density increases with ADASCs, especially when combined with a corneal stromal lamina.[105,109] Other approaches include decellularized human stromal lamina implantation, allogenic SMILE lenticules, recombinant crosslinked collagen implants, and bioengineered corneal constructs.[110]

Scheimpflug imaging and AS-OCT help objectively assess corneal transparency post-therapy. IVCM shows that initially rounded ADASCs gradually adopt a spindle-like morphology, similar to native keratocytes, increasing density in both anterior and posterior stroma.[105,106,111] While some complications like refractive errors and topographic irregularities have been observed, these techniques hold promise for enhancing corneal transparency and biomechanical stability.[107,109]

Integrating IVCM with regenerative therapies provides in vivo, longitudinal evaluations, facilitating qualitative and quantitative assessments of implanted cells and their integration with host tissue. This approach is crucial for optimizing corneal regeneration and tailoring treatments to individual patient needs.

Conclusions

Training in corneal confocal microscopy (IVCM) interpretation should include comprehensive resources that bridge theoretical knowledge and practical application. Visual guides that illustrate normal and pathological corneal structures are essential for hands-on learning. Additionally, it is crucial to incorporate both technical aspects and clinical applications of IVCM to provide a well-rounded foundation. Combining historical studies with recent advancements ensures a robust training approach, enabling new ophthalmologists to accurately interpret IVCM images and integrate the technology into clinical practice.[14,69,112–115]

Despite significant progress, challenges remain in the broader implementation of IVCM in routine practice. Its complexity necessitates specialized training to ensure correct interpretation. This manuscript has carefully selected references useful for initial training, emphasizing those that address both image acquisition techniques and cellular-level interpretation. Continued research is essential to establish standardized IVCM protocols across clinical settings and to enhance training for future ophthalmologists.[116]

Technological improvements could also expand IVCM's potential. Integrating wide-field real-time imaging and precise localization, similar to optical coherence tomography (OCT), could improve longitudinal follow-up of corneal pathology. However, challenges such as corneal curvature and transparency currently limit wide-field imaging. Additionally, developing non-contact procedures would enhance patient comfort.

Artificial intelligence (AI) integration into IVCM offers the potential to improve segmentation and detection of immune cells and corneal nerves, increasing efficiency and accuracy. While there are currently no ethical issues with IVCM use, incorporating AI in the future could raise concerns related to data bias, algorithm transparency, and patient safety. Addressing these challenges responsibly will be essential to maintaining ethical standards and prioritizing patient well-being.[117]

Looking forward, IVCM's role in modern ophthalmology will depend on technological advancements and careful evaluation of available devices to select the most suitable tools for each clinical scenario. Integrating AI into IVCM could revolutionize diagnostic accuracy and personalized treatment, ultimately improving visual outcomes and patient quality of life. As these innovations develop, prioritizing patient-centered approaches and maintaining rigorous safety standards will be essential to fully realize the benefits of IVCM in ophthalmic care.[118]

Methods for Literature Search

A comprehensive literature review was conducted to evaluate the applications of IVCM in corneal and ocular surface diseases. A PubMed search was conducted using the following keywords: "in vivo confocal microscopy", "corneal imaging", "ocular surface diseases", "keratitis", and "regenerative medicine". Articles published within the last seven years were prioritized, focusing on studies with clinical relevance, robust methodologies, and validated findings. Of the initial 1835 studies retrieved, 51 were selected after screening titles, abstracts, and full texts. Inclusion criteria encompassed studies investigating IVCM's role in the diagnosis, monitoring, and management of corneal pathologies, including keratitis, dystrophies, and nerve regeneration post-surgery. Data extraction emphasized IVCM's diagnostic accuracy, technical advancements, and clinical applications.

Ethics Approval

The Ethics, Research, and Biohazard Committees of Instituto de Oftalmología Fundación Conde de Valenciana IAP approved this study.

Author Contributions

All authors made a significant contribution to the work reported, whether that is in the conception, study design, execution, acquisition of data, analysis and interpretation, or in all these areas; took part in drafting, revising or critically reviewing the article; gave final approval of the version to be published; have agreed on the journal to which the article has been submitted; and agree to be accountable for all aspects of the work.

Funding

There is no funding to report.

Disclosure

The authors have no relevant financial or nonfinancial interests to disclose in this work.

References

1. Niederer RL, McGhee CNJ. Clinical in vivo confocal microscopy of the human cornea in health and disease. *Prog Retin Eye Res*. 2010;29(1):30–58. doi:10.1016/j.preteyeres.2009.11.001
2. Cruzat A, Qazi Y, Hamrah P. In vivo confocal microscopy of corneal nerves in health and disease. *Ocul Surf*. 2017;15(1):15–47. doi:10.1016/j.jtos.2016.09.004
3. Baratz KH, McLaren JW, Maguire LJ, Patel SV. Corneal haze determined by confocal microscopy 2 years after Descemet stripping with endothelial keratoplasty for Fuchs corneal dystrophy. *Arch Ophthalmol*. 2012;130(7):868–874. doi:10.1001/archophthalmol.2012.73
4. Guthoff RF, Zhivov A, Stachs O. In vivo confocal microscopy, an inner vision of the cornea - a major review. *Clin Experiment Ophthalmol*. 2009;37(1):100–117. doi:10.1111/j.1442-9071.2009.02016.x
5. Ramírez Fernández M. *Microscopía Confocal de La Córnea*. Vol. 1. Asociación para Evitar la Ceguera en México, I.A.P. Hospital "Dr. Luis Sánchez Bulnes"; 2022.
6. Kobayashi A, Yokogawa H, Yamazaki N, Masaki T, Sugiyama K. In vivo laser confocal microscopy after descemet's membrane endothelial keratoplasty. *Ophthalmology*. 2013;120(5):923–930. doi:10.1016/j.ophtha.2012.11.006
7. Chen T, Li Q, Tang X, Liao M, Wang H. In vivo confocal microscopy of cornea in patients with terrien's marginal corneal degeneration. *J Ophthalmol*. 2019;2019:3161843. doi:10.1155/2019/3161843
8. Kymionis GD, Diakonis VF, Shehadeh MM, Pallikaris AI, Pallikaris IG. Anterior segment applications of in vivo confocal microscopy. *Semin Ophthalmol*. 2015;30(4):243–251. doi:10.3109/08820538.2013.839817
9. Sweeney DF, Millar TJ, Raju SR. Tear film stability: a review. *Exp Eye Res*. 2013;117:28–38. doi:10.1016/j.exer.2013.08.010
10. Lee OL, Tepelus TC, Huang J, et al. Evaluation of the corneal epithelium in non-Sjögren's and Sjögren's dry eyes: an in vivo confocal microscopy study using HRT III RCM. *BMC Ophthalmol*. 2018;18(1):309. doi:10.1186/s12886-018-0971-3
11. Erdélyi B, Kraak R, Zhivov A, Guthoff R, Németh J. In vivo confocal laser scanning microscopy of the cornea in dry eye. *Graefes Arch Clin Exp Ophthalmol*. 2007;245(1):39–44. doi:10.1007/s00417-006-0375-6
12. Zhang X, Chen Q, Chen W, Cui L, Ma H, Lu F. Tear dynamics and corneal confocal microscopy of subjects with mild self-reported office dry eye. *Ophthalmology*. 2011;118(5):902–907. doi:10.1016/j.ophtha.2010.08.033
13. Guthoff RF, Wienss H, Hahnel C, Wree A. Epithelial innervation of human cornea: a three-dimensional study using confocal laser scanning fluorescence microscopy. *Cornea*. 2005;24(5):608–613. doi:10.1097/01.ico.0000154384.05614.8f
14. Petroll WM, Robertson DM. In vivo confocal microscopy of the cornea: new developments in image acquisition, reconstruction, and analysis using the HRT-Rostock corneal module. *Ocul Surf*. 2015;13(3):187–203. doi:10.1016/j.jtos.2015.05.002
15. Allgeier S, Zhivov A, Eberle F, et al. Image reconstruction of the subbasal nerve plexus with in vivo confocal microscopy. *Invest Ophthalmol Vis Sci*. 2011;52(9):5022–5028. doi:10.1167/iovs.10-6065
16. Tavakoli M, Kallinikos P, Iqbal A, et al. Corneal confocal microscopy detects improvement in corneal nerve morphology with an improvement in risk factors for diabetic neuropathy. *Diabet Med*. 2011;28(10):1261–1267. doi:10.1111/j.1464-5491.2011.03372.x
17. Stachs O, Zhivov A, Kraak R, Hovakimyan M, Wree A, Guthoff R. Structural-functional correlations of corneal innervation after LASIK and penetrating keratoplasty. *J Refract Surg*. 2010;26(3):159–167. doi:10.3928/1081597X-20100224-01
18. Kobayashi A, Yokogawa H, Sugiyama K. In vivo laser confocal microscopy of Bowman's layer of the cornea. *Ophthalmology*. 2006;113(12):2203–2208. doi:10.1016/j.ophtha.2006.05.058
19. Jalbert I, Stapleton F, Papas E, Sweeney DF, Coroneo M. In vivo confocal microscopy of the human cornea. *Br J Ophthalmol*. 2003;87(2):225–236. doi:10.1136/bjo.87.2.225
20. MeenakshiSundaram S, Sufi AR, Prajna NV, Keenan JD. Comparison of in vivo confocal microscopy, ultrasonic pachymetry, and scheimpflug topography for measuring central corneal thickness. *JAMA Ophthalmol*. 2016;134(9):1057–1059. doi:10.1001/jamaophthalmol.2016.2183
21. Efron N, Al-Dossari M, Pritchard N. In vivo confocal microscopy of the palpebral conjunctiva and tarsal plate. *Optom Vis Sci*. 2009;86(11):E1303–8. doi:10.1097/OPX.0b013e3181bc652e
22. Fasanella V, Agnifili L, Mastropasqua R, et al. In vivo laser scanning confocal microscopy of human meibomian glands in aging and ocular surface diseases. *Biomed Res Int*. 2016;2016:7432131. doi:10.1155/2016/7432131
23. Galor A, Moein HR, Lee C, et al. Neuropathic pain and dry eye. *Ocul Surf*. 2018;16(1):31–44. doi:10.1016/j.jtos.2017.10.001
24. Craig JP, Nelson JD, Azar DT, et al. TFOS DEWS II report executive summary. *Ocul Surf*. 2017;15(4):802–812. doi:10.1016/j.jtos.2017.08.003
25. Matsumoto Y, Ibrahim OMA. Application of in vivo confocal microscopy in dry eye disease. *Invest Ophthalmol Vis Sci*. 2018;59(14):DES41–DES47. doi:10.1167/iovs.17-23602
26. Villani E, Galimberti D, Viola F, Mapelli C, Ratiglia R. The cornea in Sjogren's syndrome: an in vivo confocal study. *Invest Ophthalmol Vis Sci*. 2007;48(5):2017–2022. doi:10.1167/iovs.06-1129
27. Villani E, Galimberti D, Viola F, Mapelli C, Del Papa N, Ratiglia R. Corneal involvement in rheumatoid arthritis: an in vivo confocal study. *Invest Ophthalmol Vis Sci*. 2008;49(2):560–564. doi:10.1167/iovs.07-0893
28. Lin H, Li W, Dong N, et al. Changes in corneal epithelial layer inflammatory cells in aqueous tear-deficient dry eye. *Invest Ophthalmol Vis Sci*. 2010;51(1):122–128. doi:10.1167/iovs.09-3629
29. Khamar P, Nair AP, Shetty R, et al. Dysregulated tear fluid nociception-associated factors, corneal dendritic cell density, and vitamin D levels in evaporative dry eye. *Invest Ophthalmol Vis Sci*. 2019;60(7):2532–2542. doi:10.1167/iovs.19-26914

30. Shetty R, Sethu S, Deshmukh R, et al. Corneal dendritic cell density is associated with subbasal nerve plexus features, ocular surface disease index, and serum vitamin D in evaporative dry eye disease. *Biomed Res Int*. 2016;2016:4369750. doi:10.1155/2016/4369750
31. Yang AY, Chow J, Liu J. Corneal innervation and sensation: the eye and beyond. *Yale J Biol Med*. 2018;91(1):13–21.
32. Patel S, Hwang J, Mehra D, Galor A. Corneal nerve abnormalities in ocular and systemic diseases. *Exp Eye Res*. 2021;202:108284. doi:10.1016/j.exer.2020.108284
33. Oliveira-Soto L, Efron N. Morphology of corneal nerves using confocal microscopy. *Cornea*. 2001;20(4):374–384. doi:10.1097/00003226-200105000-00008
34. Deng SX, Sejpal KD, Tang Q, Aldave AJ, Lee OL, Yu F. Characterization of limbal stem cell deficiency by in vivo laser scanning confocal microscopy: a microstructural approach. *Arch Ophthalmol*. 2012;130(4):440–445. doi:10.1001/archophthalmol.2011.378
35. Kate A, Basu S. A review of the diagnosis and treatment of limbal stem cell deficiency. *Front Med*. 2022;9:836009. doi:10.3389/fmed.2022.836009
36. Banayan N, Georgeon C, Grieve K, Ghoubay D, Baudouin F, Borderie V. In vivo confocal microscopy and optical coherence tomography as innovative tools for the diagnosis of limbal stem cell deficiency. *J Fr Ophtalmol*. 2018;41(9):e395–e406. doi:10.1016/j.jfo.2018.09.003
37. Chidambaranathan GP, Mathews S, Panigrahi AK, Mascarenhas J, Prajna NV, Muthukkaruppan V. In vivo confocal microscopic analysis of limbal stroma in patients with limbal stem cell deficiency. *Cornea*. 2015;34(11):1478–1486. doi:10.1097/ICO.0000000000000593
38. Nubile M, Lanzini M, Miri A, et al. In vivo confocal microscopy in diagnosis of limbal stem cell deficiency. *Am J Ophthalmol*. 2013;155(2):220–232. doi:10.1016/j.ajo.2012.08.017
39. Miri A, Alomar T, Nubile M, et al. In vivo confocal microscopic findings in patients with limbal stem cell deficiency. *Br J Ophthalmol*. 2012;96(4):523–529. doi:10.1136/bjophthalmol-2011-300551
40. Chan EH, Chen L, Yu F, Deng SX. Epithelial thinning in limbal stem cell deficiency. *Am J Ophthalmol*. 2015;160(4):669–77.e4. doi:10.1016/j.ajo.2015.06.029
41. Zarei-Ghanavati S, Ramirez-Miranda A, Deng SX. Limbal lacuna: a novel limbal structure detected by in vivo laser scanning confocal microscopy. *Ophthalmic Surg Lasers Imaging*. 2011;42 Online:e129–31. doi:10.3928/15428877-20111201-07
42. Erie JC, McLaren JW, Patel SV. Confocal microscopy in ophthalmology. *Am J Ophthalmol*. 2009;148(5):639–646. doi:10.1016/j.ajo.2009.06.022
43. Labbé A, Liang Q, Wang Z, et al. Corneal nerve structure and function in patients with non-Sjogren dry eye: clinical correlations. *Invest Ophthalmol Vis Sci*. 2013;54(8):5144–5150. doi:10.1167/iovs.13-12370
44. Choi EY, Kim TI, Seo KY, Kim EK, Lee HK. Corneal microstructural changes in non-Sjögren dry eye using confocal microscopy: clinical correlation. *J Korean Ophthalmol Soc*. 2015;56(5):680. doi:10.3341/jkos.2015.56.5.680
45. Villani E, Magnani F, Viola F, et al. In vivo confocal evaluation of the ocular surface morpho-functional unit in dry eye. *Optom Vis Sci*. 2013;90(6):576–586. doi:10.1097/OPX.0b013e318294c184
46. Benítez Del Castillo JM, Wasfy MAS, Fernandez C, Garcia-Sanchez J. An in vivo confocal masked study on corneal epithelium and subbasal nerves in patients with dry eye. *Invest Ophthalmol Vis Sci*. 2004;45(9):3030–3035. doi:10.1167/iovs.04-0251
47. Zhang M, Chen J, Luo L, Xiao Q, Sun M, Liu Z. Altered corneal nerves in aqueous tear deficiency viewed by in vivo confocal microscopy. *Cornea*. 2005;24(7):818–824. doi:10.1097/01.ico.0000154402.01710.95
48. Roca D, Jain S, Mun C, et al. Novel management of ocular surface inflammation in patients with ocular graft-versus-host disease in the setting of cataract surgery. *Eye Contact Lens*. 2024;50(4):189–193. doi:10.1097/ICL.0000000000001076
49. He J, Ogawa Y, Mukai S, et al. In vivo confocal microscopy evaluation of ocular surface with graft-versus-host disease-related dry eye disease. *Sci Rep*. 2017;7(1):10720. doi:10.1038/s41598-017-10237-w
50. Kheirkhah A, Qazi Y, Arnoldner MA, Suri K, Dana R. In vivo confocal microscopy in dry eye disease associated with chronic graft-versus-host disease. *Invest Ophthalmol Vis Sci*. 2016;57(11):4686–4691. doi:10.1167/iovs.16-20013
51. Steger B, Speicher L, Philipp W, Bechrakis NE. In vivo confocal microscopic characterisation of the cornea in chronic graft-versus-host disease related severe dry eye disease. *Br J Ophthalmol*. 2015;99(2):160–165. doi:10.1136/bjophthalmol-2014-305072
52. Tepelus TC, Chiu GB, Maram J, et al. Corneal features in ocular graft-versus-host disease by in vivo confocal microscopy. *Graefes Arch Clin Exp Ophthalmol*. 2017;255(12):2389–2397. doi:10.1007/s00417-017-3759-x
53. Galor A, Levitt RC, Felix ER, Martin ER, Sarantopoulos CD. Neuropathic ocular pain: an important yet underevaluated feature of dry eye. *Eye*. 2015;29(3):301–312. doi:10.1038/eye.2014.263
54. Hamrah P, Qazi Y, Shahatit B, et al. Corneal nerve and epithelial cell alterations in corneal allodynia. *An in Vivo Confocal Microscopy Case Series Ocul Surf*. 2017;15(1):139–151.
55. Oudejans L, He X, Niesters M, Dahan A, Brines M, van Velzen M. Cornea nerve fiber quantification and construction of phenotypes in patients with fibromyalgia. *Sci Rep*. 2016;6(1):23573. doi:10.1038/srep23573
56. Ramírez M, Martínez-Martínez L-A, Hernández-Quintela E, Velazco-Casapía J, Vargas A, Martínez-Lavín M. Small fiber neuropathy in women with fibromyalgia. An in vivo assessment using corneal confocal bio-microscopy. *Semin Arthritis Rheum*. 2015;45(2):214–219. doi:10.1016/j.semarthrit.2015.03.003
57. Kinard KI, Smith AG, Singleton JR, et al. Chronic migraine is associated with reduced corneal nerve fiber density and symptoms of dry eye. *Headache*. 2015;55(4):543–549. doi:10.1111/head.12547
58. Aggarwal S, Kheirkhah A, Cavalcanti BM, et al. Autologous serum tears for treatment of photoallodynia in patients with corneal neuropathy: efficacy and evaluation with in vivo confocal microscopy. *Ocul Surf*. 2015;13(3):250–262. doi:10.1016/j.jtos.2015.01.005
59. Moein HR, Akhlaq A, Dieckmann G, et al. Visualization of microneuromas by using in vivo confocal microscopy: an objective biomarker for the diagnosis of neuropathic corneal pain? *Ocul Surf*. 2020;18(4):651–656. doi:10.1016/j.jtos.2020.07.004
60. Ross AR, Al-Aqaba MA, Almaazmi A, et al. Clinical and in vivo confocal microscopic features of neuropathic corneal pain. *Br J Ophthalmol*. 2020;104(6):768–775. doi:10.1136/bjophthalmol-2019-314799
61. Abdolalizadeh P, Karimi M, Latifi G, et al. Role of different types of contact lenses in epithelial thickness. *Eye Contact Lens*. 2022;48(5):210–216. doi:10.1097/ICL.0000000000000878
62. Efron N, Perez-Gomez I, Morgan PB. Confocal microscopic observations of stromal keratocytes during extended contact lens wear. *Clin Exp Optom*. 2002;85(3):156–160. doi:10.1111/j.1444-0938.2002.tb03028.x

63. Kaufman SC, Hamano H, Beuerman RW, Laird JA, Thompson HW. Transient corneal stromal and endothelial changes following soft contact lens wear: a study with confocal microscopy. *CLAO J*. 1996;22(2):127–132.
64. Zhivov A, Stave J, Vollmar B, Guthoff R. In vivo confocal microscopic evaluation of langerhans cell density and distribution in the corneal epithelium of healthy volunteers and contact lens wearers. *Cornea*. 2007;26(1):47–54. doi:10.1097/ICO.0b013e31802e3b55
65. Gordon-Shaag A, Millodot M, Shneor E, Liu Y. The genetic and environmental factors for keratoconus. *Biomed Res Int*. 2015;2015:795738. doi:10.1155/2015/795738
66. Ghosh S, Mutalib HA, Kaur S, Ghoshal R, Retnasabapathy S. Corneal cell morphology in keratoconus: a confocal microscopic observation. *Malays J Med Sci*. 2017;24(2):44–54. doi:10.21315/mjms2017.24.2.6
67. Ramírez Fernández M, Hernández Quintela E, Naranjo Tackman R. Comparison of stromal corneal nerves between normal and keratoconus patients using confocal microscopy. *Arch Soc Esp Oftalmol*. 2014;89(8):308–312. doi:10.1016/j.oftal.2014.02.014
68. Alvani A, Hashemi H, Pakravan M, et al. Post-LASIK ectasia versus keratoconus: an in vivo confocal microscopy study. *Cornea*. 2020;39 (8):1006–1012. doi:10.1097/ICO.0000000000002318
69. Shukla AN, Cruzat A, Hamrah P. Confocal microscopy of corneal dystrophies. *Semin Ophthalmol*. 2012;27(5–6):107–116. doi:10.3109/ 08820538.2012.707276
70. Jing Y, Wang L. Morphological evaluation of Schnyder's crystalline corneal dystrophy by laser scanning confocal microscopy and Fourier-domain optical coherence tomography. *Clin Experiment Ophthalmol*. 2009;37(3):308–312. doi:10.1111/j.1442-9071.2009.02021.x
71. Kobayashi A, Fujiki K, Fujimaki T, Murakami A, Sugiyama K. In vivo laser confocal microscopic findings of corneal stromal dystrophies. *Arch Ophthalmol*. 2007;125(9):1168–1173. doi:10.1001/archopht.125.9.1168
72. Yeh SI, Liu TS, Ho CC, Cheng HC. In vivo confocal microscopy of combined pre-descemet membrane corneal dystrophy and fuchs endothelial dystrophy. *Cornea*. 2011;30(2):222–224. doi:10.1097/ICO.0b013e3181e2cf3f
73. Kobayashi A, Sugiyama K, Huang AJW. In vivo confocal microscopy in patients with central cloudy dystrophy of François. *Arch Ophthalmol*. 2004;122(11):1676–1679. doi:10.1001/archopht.122.11.1676
74. Pan F, Yao YF, Nie X, Zhang B. Clinical characteristics and in vivo confocal microscopic imaging of Fleck corneal dystrophy. *Zhejiang Da Xue Xue Bao Yi Xue Ban*. 2011;40(3):321–326. doi:10.3785/j.issn.1008-9292.2011.03.016
75. Erdem U, Muftuoglu O, Hurmeric V. In vivo confocal microscopy findings in a patient with posterior amorphous corneal dystrophy. *Clin Experiment Ophthalmol*. 2007;35(1):99–102. doi:10.1111/j.1442-9071.2007.01426.x
76. Altamirano F, Ortiz-Morales G, O'Connor-Cordova MA, Sancén-Herrera JP, Zavala J, Valdez-Garcia JE. Fuchs endothelial corneal dystrophy: an updated review. *Int Ophthalmol*. 2024;44(1):61. doi:10.1007/s10792-024-02994-1
77. Mustonen RK, McDonald MB, Srivannaboon S, Tan AL, Doubrava MW, Kim CK. In vivo confocal microscopy of Fuchs' endothelial dystrophy. *Cornea*. 1998;17(5):493–503. doi:10.1097/00003226-199809000-00006
78. Chiou AG, Kaufman SC, Beuerman RW, Maitchouk D, Kaufman HE. Confocal microscopy in posterior polymorphous corneal dystrophy. *Ophthalmologica*. 1999;213(4):211–213. doi:10.1159/000027423
79. You JY, Botelho PJ. Corneal in vivo confocal microscopy: clinical applications. *R I Med J*. 2016;99(6):30–33.
80. Kaufman SC, Musch DC, Belin MW, et al. Confocal microscopy: a report by the American Academy of Ophthalmology. *Ophthalmology*. 2004;111(2):396–406. doi:10.1016/j.ophtha.2003.12.002
81. Austin A, Lietman T, Rose-Nussbaumer J. Update on the management of infectious keratitis. *Ophthalmology*. 2017;124(11):1678–1689. doi:10.1016/j.ophtha.2017.05.012
82. Hsiao YC, Tsai IL, Kuo CT, Yang TL. Diagnosis of microsporidial keratitis with in vivo confocal microscopy. *J Xray Sci Technol*. 2013;21 (1):103–110.
83. Cañadas P, García-Gonzalez M, Cañones-Zafra R, Teus MA. Corneal confocal microscopy findings in neuro lyme disease: a case report. *Diagnostics*. 2022;12(2):343. doi:10.3390/diagnostics12020343
84. Kaufman SC, Laird JA, Cooper R, Beuerman RW. Diagnosis of bacterial contact lens related keratitis with the white-light confocal microscope. *CLAO J*. 1996;22(4):274–277.
85. Sutphin JE, Kantor AL, Mathers WD, Mehaffey MG. Evaluation of infectious crystalline keratitis with confocal microscopy in a case series. *Cornea*. 1997;16(1):21–26.
86. Gupta N, Ganger A, Bhartiya S, Verma M, Tandon R. In vivo confocal microscopic characteristics of crystalline keratopathy in patients with sclerokeratitis. *Ocul Immunol Inflamm*. 2018;26(5):700–705. doi:10.1080/09273948.2017.1281422
87. Su PY, Hu FR, Chen YM, Han JH, Chen WL. Dendritiform cells found in central cornea by in-vivo confocal microscopy in a patient with mixed bacterial keratitis. *Ocul Immunol Inflamm*. 2006;14(4):241–244. doi:10.1080/09273940600732398
88. Wang YE, Tepelus TC, Vickers LA, et al. Role of in vivo confocal microscopy in the diagnosis of infectious keratitis. *Int Ophthalmol*. 2019;39 (12):2865–2874. doi:10.1007/s10792-019-01134-4
89. Bourcier T, Dupas B, Borderie V, et al. Heidelberg retina tomograph II findings of Acanthamoeba keratitis. *Ocul Immunol Inflamm*. 2005;13 (6):487–492. doi:10.1080/09273940590951098
90. Chiou AG, Kaufman SC, Beuerman RW, Ohta T, Kaufman HE. Differential diagnosis of linear corneal images on confocal microscopy. *Cornea*. 1999;18(1):63–66. doi:10.1097/00003226-199901000-00011
91. Garcia-Gonzalez M, Cañadas P, Gros-Otero J, et al. Long-term corneal subbasal nerve plexus regeneration after laser in situ keratomileusis. *J Cataract Refract Surg*. 2019;45(7):966–971. doi:10.1016/j.jcrs.2019.02.019
92. Ramírez M, Hernández-Quintela E, Naranjo-Tackman R. A comparative confocal microscopy analysis after LASIK with the IntraLase femtosecond laser vs hansatome microkeratome. *J Refract Surg*. 2007;23(3):305–307. doi:10.3928/1081-597X-20070301-15
93. Ramírez M, Hernández-Quintela E, Sánchez-Huerta V, Naranjo-Tackman R. Confocal microscopy of corneal flap microfolds after LASIK. *J Refract Surg*. 2006;22(2):155–158. doi:10.3928/1081-597X-20060201-13
94. Bilgihan K, Yesilirmak N, Altay Y, et al. Evaluation of long-term corneal morphology after photorefractive keratectomy by in vivo confocal microscopy and specular microscopy; 20-year follow-up. *Eye Contact Lens*. 2019;45(6):360–364. doi:10.1097/ICL.0000000000000585
95. Tomás-Juan J, Murueta-Goyena Larrañaga A, Hanneken L. Corneal regeneration after photorefractive keratectomy: a review. *J Optom*. 2015;8 (3):149–169. doi:10.1016/j.optom.2014.09.001

96. Liu M, Zhang T, Zhou Y, et al. Corneal regeneration after femtosecond laser small-incision lenticule extraction: a prospective study. *Graefes Arch Clin Exp Ophthalmol*. 2015;253(7):1035–1042. doi:10.1007/s00417-015-2971-9
97. Agca A, Cankaya KI, Yilmaz I, et al. Fellow eye comparison of nerve fiber regeneration after SMILE and femtosecond laser-assisted LASIK: a confocal microscopy study. *J Refract Surg*. 2015;31(9):594–598. doi:10.3928/1081597X-20150820-04
98. Agca A, Ozgurhan EB, Yildirim Y, et al. Corneal backscatter analysis by in vivo confocal microscopy: fellow eye comparison of small incision lenticule extraction and femtosecond laser-assisted LASIK. *J Ophthalmol*. 2014;2014:265012. doi:10.1155/2014/265012
99. Recchioni A, Sisó-Fuertes I, Hartwig A, et al. Short-term impact of FS-LASIK and SMILE on dry eye metrics and corneal nerve morphology. *Cornea*. 2020;39(7):851–857. doi:10.1097/ICO.0000000000002312
100. Ramírez M, Cabrera E, La Torre-González ED, Hernández-Quintela E. In vivo confocal microscopy findings after SMILE refractive surgery technique. *Cir Cir*. 2021;89(5):570–573. doi:10.24875/CIRU.21000026
101. Mazzotta C, Hafezi F, Kymionis G, et al. In vivo confocal microscopy after corneal collagen crosslinking. *Ocul Surf*. 2015;13(4):298–314. doi:10.1016/j.jtos.2015.04.007
102. Darwish T, Brahma A, Efron N, O'Donnell C. Subbasal nerve regeneration after penetrating keratoplasty. *Cornea*. 2007;26(8):935–940. doi:10.1097/ICO.0b013e3180de493f
103. Schiano-Lomoriello D, Colabelli-Gisoldi RA, Nubile M, et al. Descemetic and predescemetic DALK in keratoconus patients: a clinical and confocal perspective study. *Biomed Res Int*. 2014;2014:123156. doi:10.1155/2014/123156
104. Ramírez M, Ortiz C, Dewit-Carter G, Hernández-Quintela E. Confocal microscopy findings after endothelial transplant by DSAEK. *Cir Cir*. 2018;86(2):128–131. doi:10.24875/CIRU.M18000020
105. Alió JL, Alió Del Barrio JL, El Zarif M, et al. Regenerative surgery of the corneal stroma for advanced keratoconus: 1-year outcomes. *Am J Ophthalmol*. 2019;203:53–68. doi:10.1016/j.ajo.2019.02.009
106. Del Barrio JL A, El Zarif M, de Miguel MP, et al. Cellular therapy with human autologous adipose-derived adult stem cells for advanced keratoconus. *Cornea*. 2017;36(8):952–960. doi:10.1097/ICO.0000000000001228
107. Espandar L, Bunnell B, Wang GY, Gregory P, McBride C, Moshirfar M. Adipose-derived stem cells on hyaluronic acid–derived scaffold: a new horizon in bioengineered cornea. *Arch Ophthalmol*. 2012;130(2):202–208. doi:10.1001/archopthalmol.2011.1398
108. Arnalich-Montiel F, Pastor S, Blazquez-Martinez A, et al. Adipose-derived stem cells are a source for cell therapy of the corneal stroma. *Stem Cells*. 2008;26(2):570–579. doi:10.1634/stemcells.2007-0653
109. El Zarif M, A Jawad K, Alió Del Barrio JL, et al. Corneal stroma cell density evolution in keratoconus corneas following the implantation of adipose mesenchymal stem cells and corneal laminas: an in vivo confocal microscopy study. *Invest Ophthalmol Vis Sci*. 2020;61(4):22. doi:10.1167/iovs.61.4.22
110. El Zarif M, Alió JL, Alió Del Barrio JL, De Miguel MP, Abdul Jawad K, Makdissy N. Corneal stromal regeneration: a review of human clinical studies in keratoconus treatment. *Front Med*. 2021;8:650724. doi:10.3389/fmed.2021.650724
111. van Dijk K, Liarakos VS, Parker J, et al. Bowman layer transplantation to reduce and stabilize progressive, advanced keratoconus. *Ophthalmology*. 2015;122(5):909–917. doi:10.1016/j.ophtha.2014.12.005
112. Guthoff RF, Baudouin C, Stave J. Confocal laser scanning in vivo microscopy. In: Guthoff RF, Baudouin C, Stave J, editors. *Atlas of Confocal Laser Scanning In-Vivo Microscopy in Ophthalmology: Principles and Applications in Diagnostic and Therapeutic Ophthalmology*. Berlin Heidelberg: Springer; 2006:31–148.
113. Masters BR, Thaer AA. In-vivo real-time confocal microscopy of the human cornea. In: *Ophthalmic Technologies III*. Vol. 1877. SPIE; 1993:100–121.
114. Masters BR, Thaer AA. Real-time scanning slit confocal microscopy of the in vivo human cornea. *Appl Opt*. 1994;33(4):695–701. doi:10.1364/AO.33.000695
115. Böhnke M, Masters BR. Confocal microscopy of the cornea. *Prog Retin Eye Res*. 1999;18(5):553–628. doi:10.1016/S1350-9462(98)00028-7
116. Chew SJ, Beuerman RW, Assouline M, Kaufman HE, Barron BA, Hill JM. Early diagnosis of infectious keratitis with in vivo real time confocal microscopy. *CLAO J*. 1992;18(3):197–201.
117. Pfister DR, Douglas Cameron J, Krachmer JH, Holland EJ. Confocal microscopy findings of acanthamoeba keratitis. *Am J Ophthalmol*. 1996;121(2):119–128. doi:10.1016/s0002-9394(14)70576-8
118. El Zarif M, Alió Del Barrio JL, Mingo D, A Jawad K, Alió JL. Corneal stromal densitometry evolution in a clinical model of cellular therapy for advanced keratoconus. *Cornea*. 2023;42(3):332–343. doi:10.1097/ICO.0000000000003152